BMC Microbiology

RESEARCH Open Access

Gut microbiota and relevant metabolites analysis in perianal abscess of infants

Shuai Wang[1], Jingfeng Zhang[1], Mingfeng Fan[1], Zhenmei Dong[2], Laian Li[1], Juan Xu[1], Wanbin Yin[1*] and Xiangjun Xu[1*]

Abstract

Objectives To explore the characteristics of the gut microbiota and metabolites in infants with perianal abscess compared with healthy infants, thereby providing a reference for treating perianal abscess in infants.

Methods The gut microbiota of 19 infants with perianal abscess and 21 healthy infants were compared using 16S rRNA gene sequencing. Metabolite compositions were compared between a subset of 16 infants with perianal abscess and 8 healthy infants.

Results Both groups showed significant differences in the abundance of the genera *Ruminococcus* ($P=0.002$) and *Parasutterella* ($P=0.004$). Five metabolic pathways, namely, steroid biosynthesis, one-carbon pool by folate, synthesis, secretion, and action of the parathyroid hormone, cholesterol metabolism, and tuberculosis, were significantly enriched. Three metabolites, namely, calcidiol, dihydrofolic acid, and taurochenodesoxycholic acid, were involved in these enriched pathways.

Conclusion The study revealed significant differences in the composition of the gut microbiota and metabolites between healthy infants and those with perianal abscess, suggesting a potential association between the gut microbiota and infantile perianal abscess.

Keywords Perianal abscess, Infant, Gut microbiota, Metabolites

Introduction

Perianal abscesses are predominantly caused by anal gland infections, which spread upward and downward, leading to acute or chronic suppurative inflammation [1]. If not treated promptly, perianal abscesses may also cause systemic infections [2, 3]. In medical practice, the predominant approach for managing perianal abscesses in adult patients is through the procedure of incision and drainage [4]. However, the management of infant perianal abscess remains contentious. Since 1998, studies have indicated that perianal abscess in infants, with a male predominance (> 93.6%), is a time-limited, self-limiting condition [5, 6]. These studies reported that nonsurgical treatment of infant perianal abscess was safe and effective. Our previous research also showed that conservative treatment of infants with perianal abscess results in an overall high success rate of 90.3% (139/153) [7].

The gut microbiota is of particular importance for the maintenance of human health. The gut microbiota has both a protective and trophic role influencing several homeostatic processes of the host organism, e.g., tissue trophism, immune balance, metabolic activity, neuroendocrine function, etc. [8, 9]. In the context of medical research, dysbiosis of the gut microbiota is recognized

*Correspondence:
Wanbin Yin
jyfyywb@126.com
Xiangjun Xu
jun8011jun@163.com
[1] Department of Anorectal Surgery, Affiliated Hospital of Jining Medical University, Jining 272029, China
[2] Department of Hematology, Affiliated Hospital of Jining Medical University, Jining 272029, China

as a contributing factor to a range of diseases. These include digestive system disorders, metabolic diseases, inflammatory bowel disease, irritable bowel syndrome, and autoimmune diseases [10, 11]. Previous studies have shown that gastrointestinal diseases are frequently associated with alterations in the diversity and abundance of the gut microbiota. This correlation suggests that individual microorganisms or the gut microbiota community as a whole may contribute to the development and progression of gastrointestinal diseases [12]. A recent study on the gut microbiota of adults with perianal abscess reported significant differences in the gut microbiota between healthy individuals and patients with perianal abscess, identifying Bilophila as a biomarker for the disease [13].

The intersection of microbiomics and metabolomics is an area with potential for optimization. Despite numerous reports on integrative multiomics in adults, data on children remain scarce. To our knowledge, no study has assessed changes in the gut microbiota and metabolites in infants with perianal abscess. Our study is the first to report significant differences in the gut microbiota and metabolite composition between healthy infants and those with perianal abscess. The gut microbial community in infants is dynamic and influenced by several factors, including the method of childbirth, feeding method, nutritional status, and the use of antibiotics [14, 15]. However, the gut microbiota in breastfeeding infants is relatively stable. We applied microbiome genomics and fecal metabolomics to understand changes in the gut microbiota and metabolites in infant perianal abscess and analyzed the related KEGG pathways. By assessing the abundance and diversity of the microbiota, we elucidated the role of the gut microbiota in the development and progression of infant perianal abscess, thereby providing reference values for personalized treatment with precision medicine.

Materials and methods

Study subjects

Among the infants visiting our hospital between May 2022 and August 2022, 19 infants with perianal abscess were categorized into Group A, while 21 healthy infants visiting the Department of Child Health were categorized into Group B.

The inclusion criteria for the abscess group were infants with perianal abscess or healthy infants. The exclusion criteria for this group were preterm infants, infants with significant physiological defects, those with a history of congenital diseases, and those treated with antibiotics or metabolism-related drugs within the last three months.

Ethical review and informed consent

The parents of all infants included in the study were informed about the benefits and risks by the researchers before they agreed to participate in the study by signing an informed consent form. The study was reviewed and approved by the Medical Ethics Committee of the Affiliated Hospital of Jining Medical University [approval number:NO.Y(2021)16].

Sample collection and processing

About 200 mg of fresh feces was collected from the infants in sterile fecal collection tubes. These samples were placed into 2 mL cryogenic vials that had been prelabeled and tested for low-temperature storage, immediately immersed in liquid nitrogen, and then transferred to an ultralow temperature freezer at –80 °C until further analysis. A total of 40 samples were transported on dry ice to the laboratory of Shanghai Ouyi Biomedical Technology Co., Ltd., for sequencing analysis.

DNA extraction and 16S rRNA gene amplification

DNA was extracted from the fecal samples using the MagPure Soil DNA LQ Kit (Magen, Room 502, No.16 Lianpu Street, Huangpu District, Guangzhou City) according to the manufacturer's instructions. Genomic DNA was extracted and used as the template for PCR amplification of the bacterial 16S rRNA gene. The amplification was carried out using barcode-specific primers and the high-fidelity Takara Ex Taq enzyme. The V3-V4 variable regions of the 16S rRNA gene were amplified using the universal primers 343 F (5'-TACGGRAGGCAG CAG-3') and 798R (5'-AGGGTATCTAATCCT-3'). The PCR products were analyzed by agarose gel electrophoresis, purified using AMPure XP beads, and subsequently subjected to a second round of PCR amplification. Following another purification step with AMPure XP beads, the final amplicons were quantified using the Qubit dsDNA Assay Kit (Thermo Fisher Scientific, USA).

Bioinformatics and data analysis

The sequencing was conducted by Shanghai OE Biotech Co., Ltd. (Shanghai, China) using the Illumina NovaSeq 6000 platform. Raw sequencing data were generated in FASTQ format. Paired-end reads were processed using Cutadapt software to detect and remove adapter sequences. After trimming, paired-end reads were filtering low quality sequences, denoised, merged and detect and cut off the chimera reads using DADA2 with the default parameters of QIIME2 (2020.11). At last, the software output the representative reads and the ASV abundance table. The representative read of each ASV was selected using QIIME2 package. All representative

reads were annotated and blasted against Silva database (Version 138) using q2-feature-classifier with the default parameters.

To assess sequencing depth, random subsampling was performed to evaluate the number of species represented in the sequences. A rarefaction curve was constructed based on sequencing depth and observed species richness to determine whether the dataset sufficiently reflected species diversity within the sample pool.Microbial community diversity was analyzed using QIIME2 software, with alpha diversity indices, including ACE (Abundance-based Coverage Estimator), Chao1, and Shannon indices, used to assess species richness and evenness. Beta diversity was evaluated using Principal Coordinates Analysis (PCoA). To identify and compare differentially abundant genera between the two groups, a t-test was performed, with $P < 0.05$ considered statistically significant.

Detection of metabolites using gas chromatography-mass spectrometry (GC–MS) and liquid chromatography-mass spectrometry(LC–MS)

A total of 60 mg of fecal sample was placed into a centrifuge tube, 600 μL of extraction solution was added, and grinding, vortexing, low-temperature ultrasonic extraction, and low-temperature centrifugation were performed. Then, 150 μL of the supernatant was transferred to a glass derivatization vial, and the sample was dried using a centrifugal concentrator.Subsequently, 80 μL of methoxyamine hydrochloride in pyridine solution (15 mg/mL) was added to the glass derivatization vial, and the mixture was incubated in a shaking incubator at 37 °C for 60 min for oximation. After removing the sample, 50 μL of BSTFA derivatization reagent and 20 μL of n-hexane were added along with 10 μL of each of the 10 internal standards, and the reaction was performed at 70 °C for 60 min. The sample was then left undisturbed at room temperature for 30 min before proceeding to GC–MS metabolomic analysis.

Of the fecal sample, 60 mg was placed into a centrifuge tube, 600μL of extraction solution was added and the sample was ground, vortexed, subjected to low-temperature ultrasonic extraction, and subjected to low-temperature centrifugation. Then, 150 μL of the supernatant was aspirated using a syringe, filtered through a 0.22 μm organic phase syringe filter, and transferred to an LC autosampler vial. Finally, the sample was stored at −80 °C until use for LC–MS metabolomics analysis.

Observe the overall distribution between samples and the stability of the entire analysis process through principal component analysis (PCA). Orthogonal Partial Least-Squares-Discriminant Analysis (OPLS-DA) was utilized to distinguish the metabolites that differ between groups. Variable Importance of Projection (VIP) values obtained from the OPLS-DA model were used to rank the overall contribution of each variable. T-test was further used to verify whether the metabolites of difference between groups were significant. Differential metabolites were selected with VIP values greater than 1.0 and p-values less than 0.05.

Results

Study subjects

A total of 40 male infants, including 19 infants with perianal abscess and 21 healthy infants, were included in this study. Baseline characteristics were similar between the 2 groups (Table 1).

Statistics and distribution of sample ASVs

A total of 1209 ASVs were collected. Based on the results of the ASV clustering analysis and the research requirements, the number of shared and specific ASVs across different samples (groups) was analyzed. These data were then visualized as a flower plot (Fig. 1).

A sharp rise in the rarefaction curve indicated insufficient sequencing depth, necessitating an increase in the sample size. A relatively flat curve indicated that the sample size was sufficient for data analysis (Fig. 2).

Sample community structure distribution

The community structure was primarily used to present the overall microbial composition, showing dominant microbial groups, among others. This structure was represented across seven levels of classification, with phylum and genus being the most commonly used. Microbial abundance is depicted as bar graphs, with the four dominant phyla being Proteobacteria, Firmicutes,

Table 1 Clinical characteristics of the infants. IQR, internal quartile range

Characteristics	*Group A (n=19)*	*Group B (n=21)*	*P value*
Male sex, *n* (%)	19 (100%)	21 (100%)	1.000
Age of presentation, median (IQR)	46 (35, 63)	43 (42, 48)	0.568
Height, median (IQR)	58 (56, 62)	58 (56, 59)	0.694
Weight, median (IQR)	5 (4.5, 7.0)	5.2 (5.0, 5.8)	0.968
Stool frenquency *n* (%)			0.056
< 5	10	17	
≥5	9	4	
Mode of delivery			0.987
Vaginal birth	9	10	
Cesarean section	10	11	
Mode of feeding			0.796
Mixed feeding	8	8	
Breast milk	11	13	

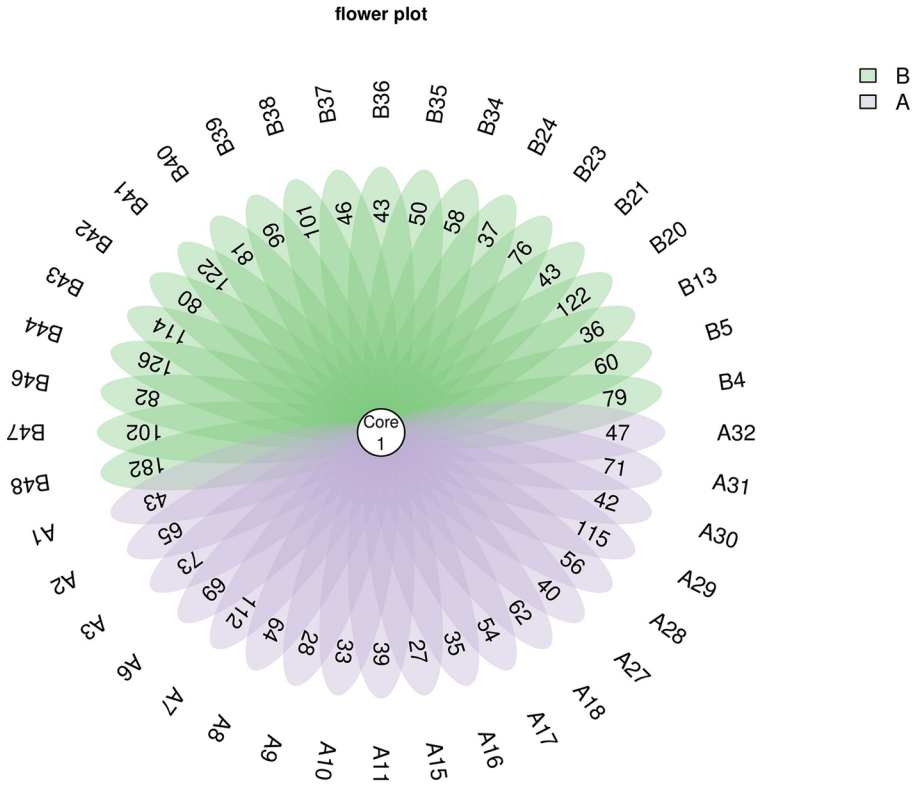

Fig. 1 Flower plot representing the number of shared and specific ASVs. The number at the core of the diagram represents the number of shared ASVs across all samples (i.e., core ASVs). The numbers on the petals indicate the total number of ASVs in each sample minus the number of shared ASVs, i.e., specific ASVs

Actinobacteria and Bacteroidetes (Fig. 3A). The top ten genera were Escherichia-Shigella, Klebsiella, Bifidobacterium, Clostridium_sensu_stricto_1, Bacteroides, Enterobacter, Citrobacter, Streptococcus, Enterococcus and Collinsella (Fig. 3B). The top 15 genera and their relative abundances in each sample individually is shown in Fig. 3C.

Analysis of sample diversity

The used indices, ACE index ($P = 0.014$), Chao1 index ($P = 0.013$) and Shannon index ($P = 0.03$) (Fig. 4), showed that the diversity of Group A was significantly lower than Group B. This finding suggested that the abundance and evenness of microbial communities varied between the two groups.

Beta diversity was primarily used to analyze the differences in microbial community diversity within and between groups. Small intragroup and large intergroup variations indicate ideal sample selection. Principal coordinate analysis (PCoA) was performed to provide results based on binary jaccard distance matrice. PERMANOVA (Permutational Multivariate Analysis of Variance) is used to examine differences between groups based on the distance matrix. The closer the samples within the same group are to each other and the more distinct they are from other groups, the better the grouping effect. A slight overlap was observed between the two groups (Fig. 5). However, a P value of 0.001 confirmed that the community composition differed significantly between the two groups.

Screening for differentially abundant genera

Among the four dominant phyla *Firmicutes* was significantly lower abundant in the abscess group than in the control group ($P = 0.015$) (Fig. 6B). Statistical analysis at the genus level was conducted to select the top 10 genera with different abundances for the analysis of relative abundance. In the abscess group, *Muribaculaceae*, *Sphingomonas* and *Clade_Ia* had greater relative abundances than did the control group, whereas *Faecalibacterium*, *[Eubacterium]_coprostanoligenes_group*, *Ruminococcus*, *Allobaculum*, *Parasutterella*, *Romboutsia* and *Neisseria* had lower relative abundances than did the control group (Fig. 6A). There were significant differences in the relative abundance of all these microorganisms, especially *Ruminococcus* ($P = 0.002$) and *Parasutterella* ($P = 0.004$) (Fig. 6B).

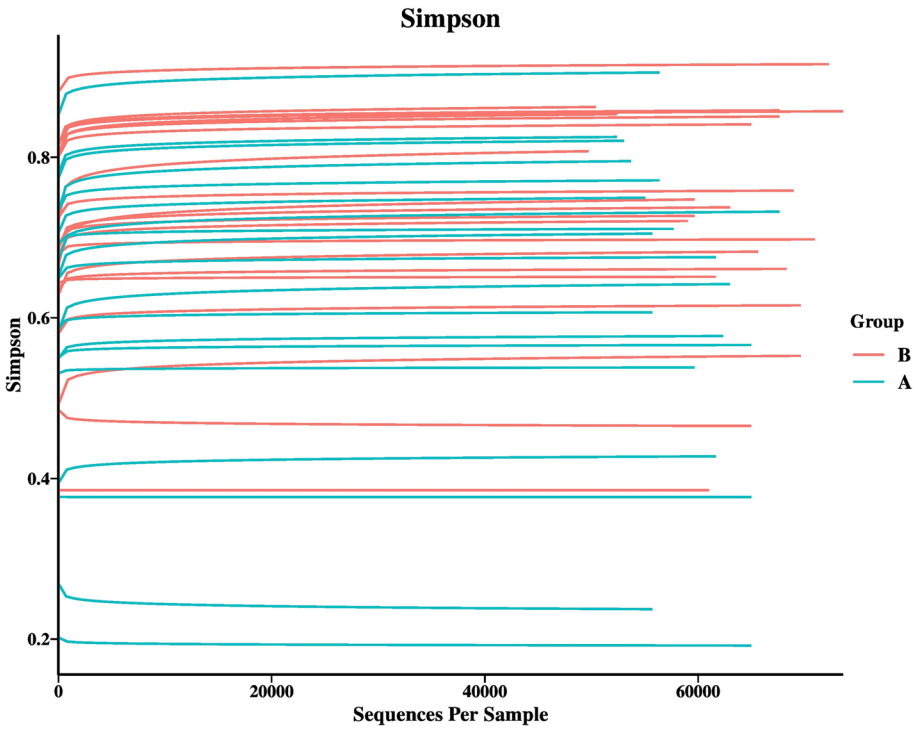

Fig. 2 Rarefaction curves constructed using sequence numbers and species. Each curve represents a sample, with the horizontal axis showing the depth of random sampling (i.e., the number of sampled sequences) and the vertical axis showing the index values. Groups A and B are represented by blue and red curves, respectively

Screening for differentially abundant metabolites and enriched pathways

A total of 107 significantly different metabolites were detected, and hierarchical clustering was performed on the expression levels of the top 50 metabolites sorted by VIP scores (Supplementary Figure S1). Among these, nine metabolites, including norlinolenic acid, zymosterol, ketoleucine, creatine, L-asparagine, taurochenodesoxycholic acid, 4-imidazolone-5-propionic acid, calcidiol and dihydrofolic acid were enriched in metabolic pathways. Analysis of the top 10 enriched metabolic pathways revealed that Steroid biosynthesis, One-carbon pool by folate, Parathyroid hormone synthesis, secretion and action, Cholesterol metabolism and Tuberculosis were the five pathways with significant enrichment of the metabolites (Fig. 7A), indicating that these pathways changed significantly in the abscess group compared with the control group. In these differential metabolic pathways, calcidiol, dihydrofolic acid, and taurochenodesoxycholic acid were the three metabolites exhibiting significant enrichment. The three metabolites were significantly lower abundant in the abscess group than in the control group (Fig. 7B).

Correlation analysis of differential microbiota and metabolites

Using Pearson correlation analysis of significantly different microbiota and metabolites between groups, the relationships between the top 100 microbial and metabolite pairs with the highest absolute correlation coefficients were visualized as a correlation network diagram (Fig. 8). If there were fewer than 100 pairs, all pairs were used. In the network diagram, nodes showing more connections with other nodes had a greater impact. *Parasutterella* was associated with 26 metabolites, showing the most connected nodes (Fig. 8). This finding indicated its important role in the development and progression of infant perianal abscess.

Discussion

This study analyzed the changes in the gut microbiota of healthy subjects and children with perianal abscess through 16S rRNA gene sequencing. The classification and composition of the gut microbiota varied significantly between the two groups. Among the four dominant phyla, *Firmicutes* was significantly lower abundant in the abscess group than in the control group. At the

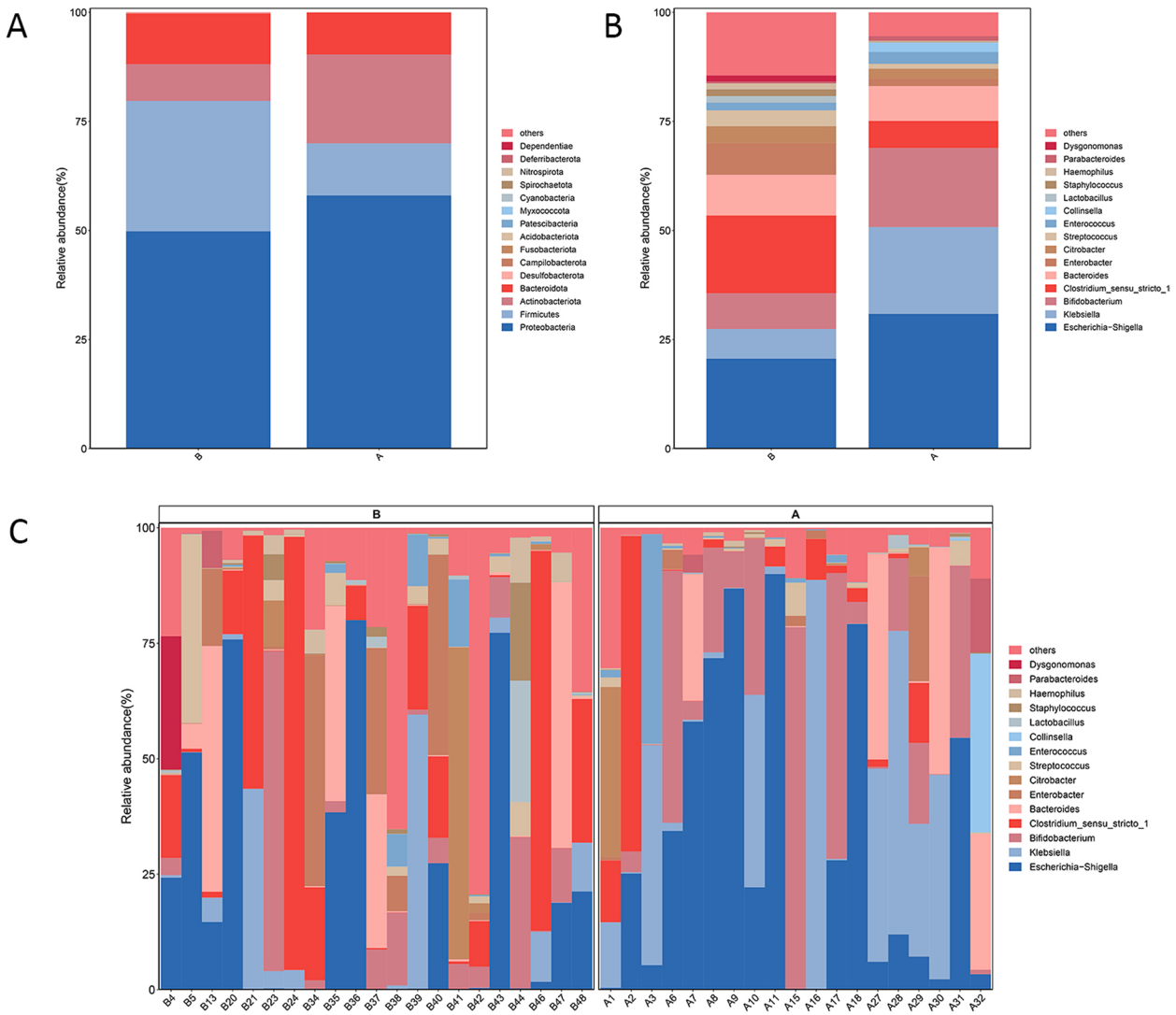

Fig. 3 **A** The top 4 predominant bacteria at the phylum level:*Proteobacteria*, *Firmicutes*, *Actinobacteria*, and Bacteroidetes; **B** The top 15 genera and their relative abundances in both groups; **C** The top 15 genera and their relative abundances in each sample individually

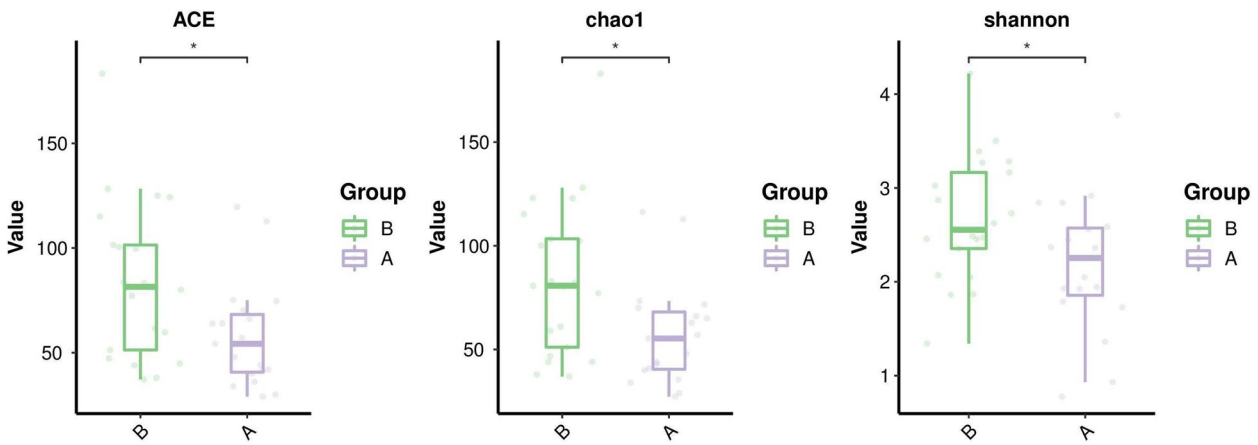

Fig. 4 Analysis of the three alpha diversity indices:the ACE index, the Chao1 index and the Shannon index between the two groups

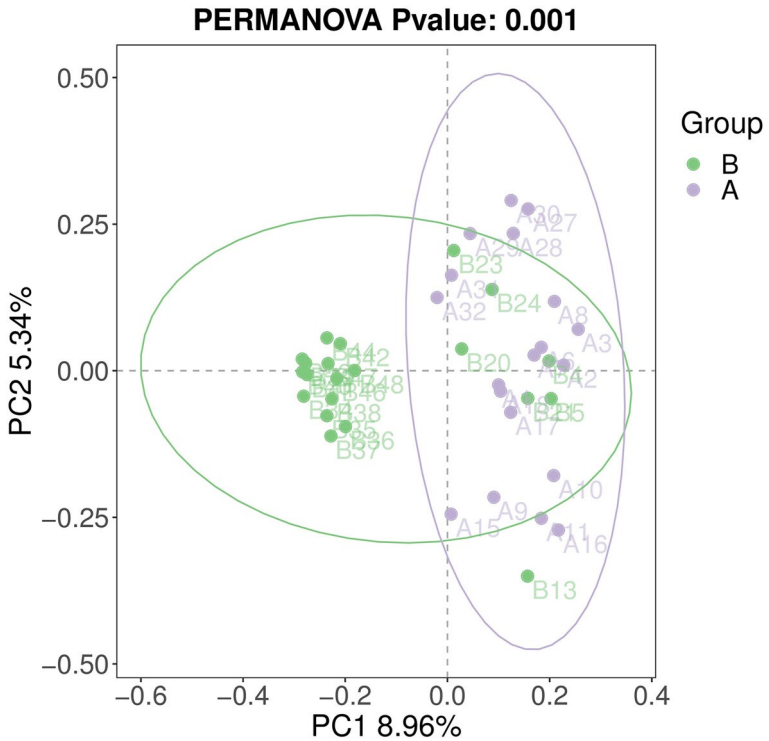

Fig. 5 The horizontal axis (PC1) and the vertical axis (PC2) represent the two principal coordinates explaining the maximum variance in differences between samples. Samples from the same group are marked with the same color, with each point representing an individual sample. Similar samples are clustered together

genus level, a total of 10 gut microbial genera were validated, which could differentiate the healthy infants from the infants with perianal abscess. *Ruminococcus* (*R. gnavus*) and *Parasutterella* had the most significant differences in abundance. Therefore, *R. gnavus* and *Parasutterella* might be used as potential biomarkers for the diagnosis of infant perianal abscess.

R. gnavus is a prevalent human gut symbiont and early colonizer of the infant gut that persists throughout adulthood. It is one of 57 bacterial species that occurs in more than 90% of individuals, with a median abundance of 0.1% across populations [16]. Although this bacterium is typically a beneficial component of the normal microbiota, recent findings have linked it to a growing number of intestinal and extraintestinal diseases [17]. Bile acid metabolites have been implicated in the role of *R. gnavus* not only in inflammation and metabolic disorders but also in the development of neurological or psychological disorders [18]. The comparison of the functional differences in the gut microbiota between healthy infants and those with perianal abscess revealed that calcidiol is involved in the enrichment of the steroid biosynthesis pathway, and taurochenodeoxycholic acid participates in the enrichment of the cholesterol metabolism pathway. This finding highlights the role of bile acids in the development and progression of infant perianal abscess. However, we did not observe a direct correlation between *R. gnavus* and bile acid metabolites. This does not rule out the possibility that *R. gnavus* may influence bile acid metabolism through other pathways, necessitating further confirmation.

The abundance of *Parasutterella*, another genus whose abundance significantly differed between the two groups, was closely related to the abundance of differentially abundant metabolites according to correlation analysis. This genus is a member of the healthy fecal core microbiome in the human gastrointestinal tract [19]. The relative abundance of this bacterium has been associated with various host health outcomes, such as inflammatory bowel disease, obesity, diabetes and fatty liver disease [20, 21]. Research has demonstrated that *Parasutterella* produces succinate as a fermentation end product and affects the metabolism of purines, tryptophan and bile acids. We also observed that *Parasutterella* had varying degrees of correlation with the above metabolites. Some studies have indicated that the accumulation of extracellular succinate leads to its increased uptake by macrophages, which activates a proinflammatory response and the release of cytokines, resulting in chronic inflammation [22]. Other investigators reported that the

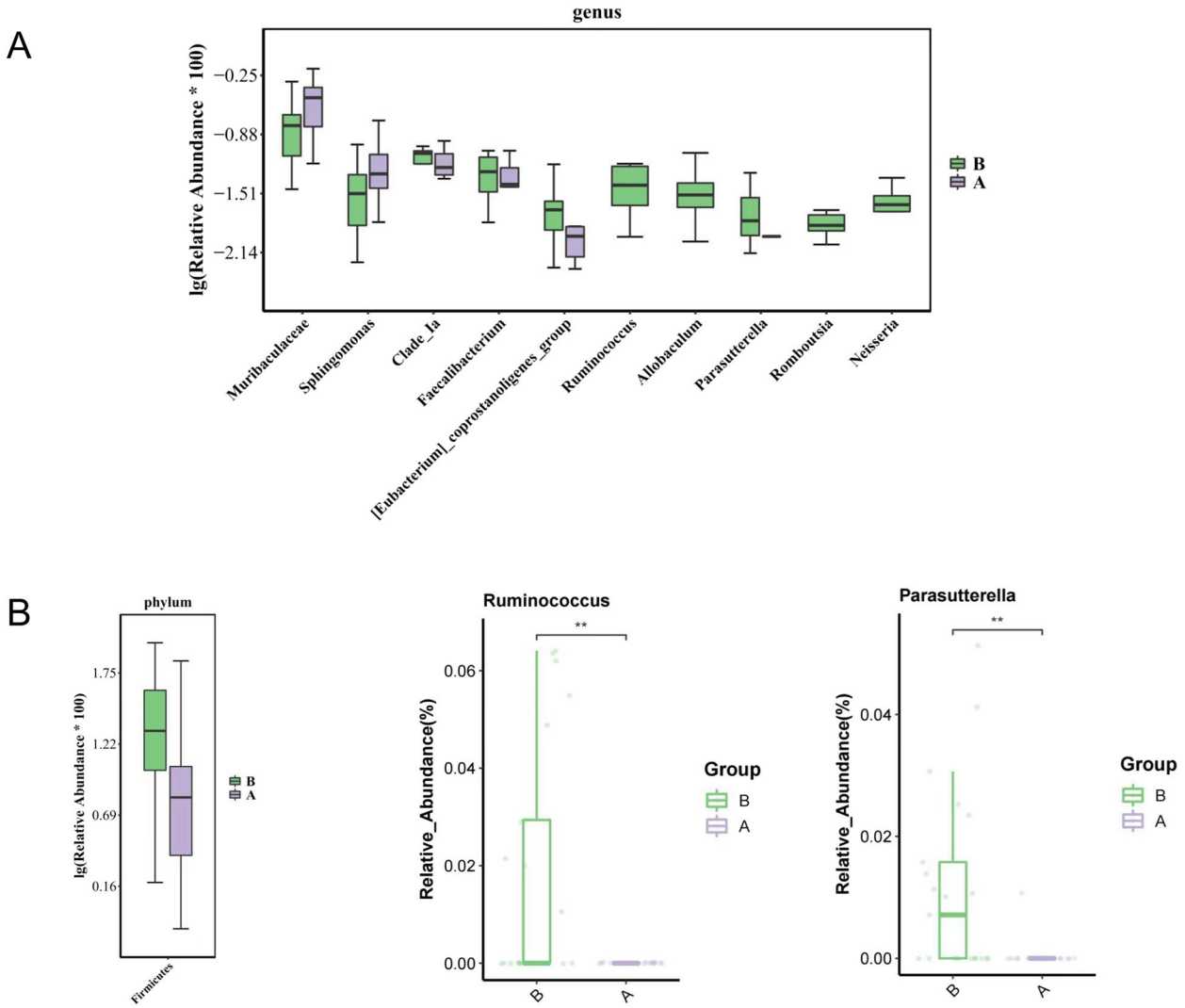

Fig. 6 **A** Analysis of the relative abundance of the top 10 most abundant species at the genus level; **B** Relative abundances of *Firmicutes*, *Ruminococcus* and *Parasutterella* with the greatest differences in abundance between the two groups

accumulation of succinate promotes an anti-inflammatory response [23, 24]. Purine-derived metabolites have been reported to modulate the responses of immune cells and the gut mucosal barrier [25]. A study using a mouse DSS-induced colitis model demonstrated that hypoxanthine could modulate the energy balance of the intestinal epithelium and play a critical role in maintaining intestinal barrier function [26]. Tryptophan plays an important role in maintaining the homeostasis of symbiotic microorganisms, inhibiting inflammation, and regulating intestinal immune tolerance [27]. Recent data suggest that indoles produced through tryptophan metabolism play a crucial role in maintaining intestinal homeostasis and are intimately linked to intestinal microecology and overall human health [28, 29].

In addition to participating in the steroid biosynthesis pathway, calcidiol also contributes to the synthesis, secretion, and action of parathyroid hormone, as well as the tuberculosis pathway, promoting the synthesis of calcitriol. Calcitriol is the active form of vitamin D in the human body and exerts immunomodulatory effects by binding to the vitamin D receptor (VDR). VDR and CYP27B1 are expressed in most immune cells, e.g., T and B lymphocytes, monocytes, natural killer cells, and dendritic cells [30]. Vitamin D plays a critical role in the host's defense against bacterial, fungal, and viral infections by stimulating the production of antimicrobial peptides (AMPs), which act as endogenous antibiotics and are among the body's first lines of defense [31].

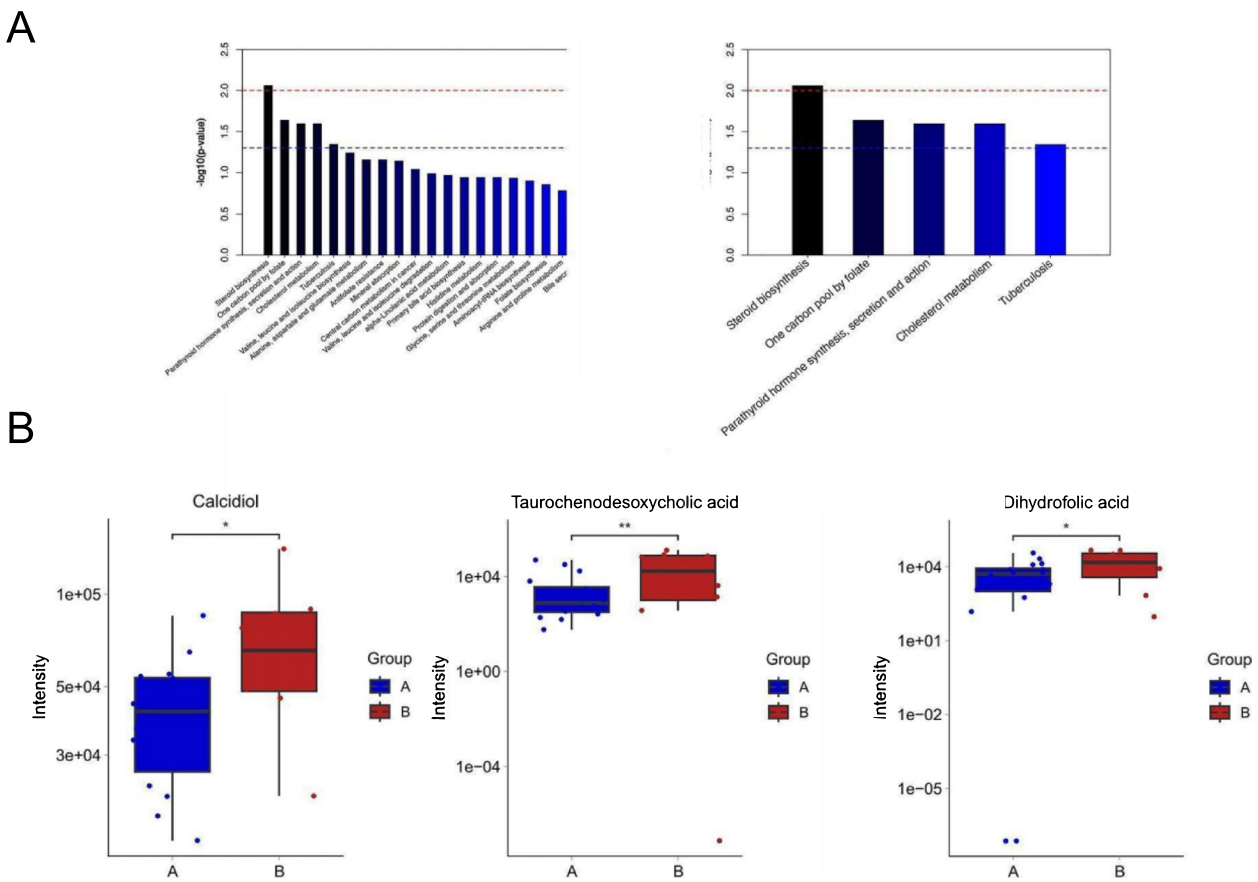

Fig. 7 **A** The left graph presents the top 10 enriched metabolic pathways, while the right graph presents the five metabolic pathways with significant differences between groups. The red line indicates a *P* value of 0.01, while the blue line indicates a *P* value of 0.05; 7 **B** Three metabolites were significantly different between the two groups

The final enriched pathway was the one-carbon pool of folate, in which dihydrofolic acid participates in the production of tetrahydrofolate (THF). THF functions as a universal one-carbon receptor. It accepts one-carbon units derived from amino acids to form formyl-THF, methyl-THF nd methylene-THF, which provide one-carbon units for purine synthesis, the methionine cycle, and the synthesis of thymidylate nucleotides, respectively [32]. The one-carbon pathway plays an important role in the methylation of nucleic acids, histones, neurotransmitters, phospholipids, proteins, homocysteine, and indirectly in the reduction of glutathione (GSH) [33]. The metabolism of one-carbon units can regulate the synthesis of nucleic acids, proteins, lipids, and maintain the redox homeostasis of the cell. GSH is a low-molecular-weight antioxidant that is present in nearly all cells and limits the impact of oxidative stress on vital cellular components such as lipids, proteins and DNA through redox reactions [34]. GSH functions as a redox sensor at the onset of DNA synthesis by maintaining the nuclear architecture, providing the appropriate redox environment for DNA replication, and safeguarding DNA integrity [35]. It is also a key regulator of epigenetic events critical for the regulation of cell proliferation and cellular resistance to apoptosis [36].

To our knowledge, this is the first study to explore the gut microbiota in infants with perianal abscess, providing important insights for future research. However, due to limitations in sample size and experimental conditions, the relationship between the gut microbiota and perianal abscess requires further investigation. In future work, we plan to address these limitations by expanding the sample size and conducting more in-depth studies.

Conclusion

The study revealed significant differences in the composition of the gut microbiota and metabolites between healthy infants and those with perianal abscess, suggesting a potential association between the gut microbiota and infantile perianal abscess.

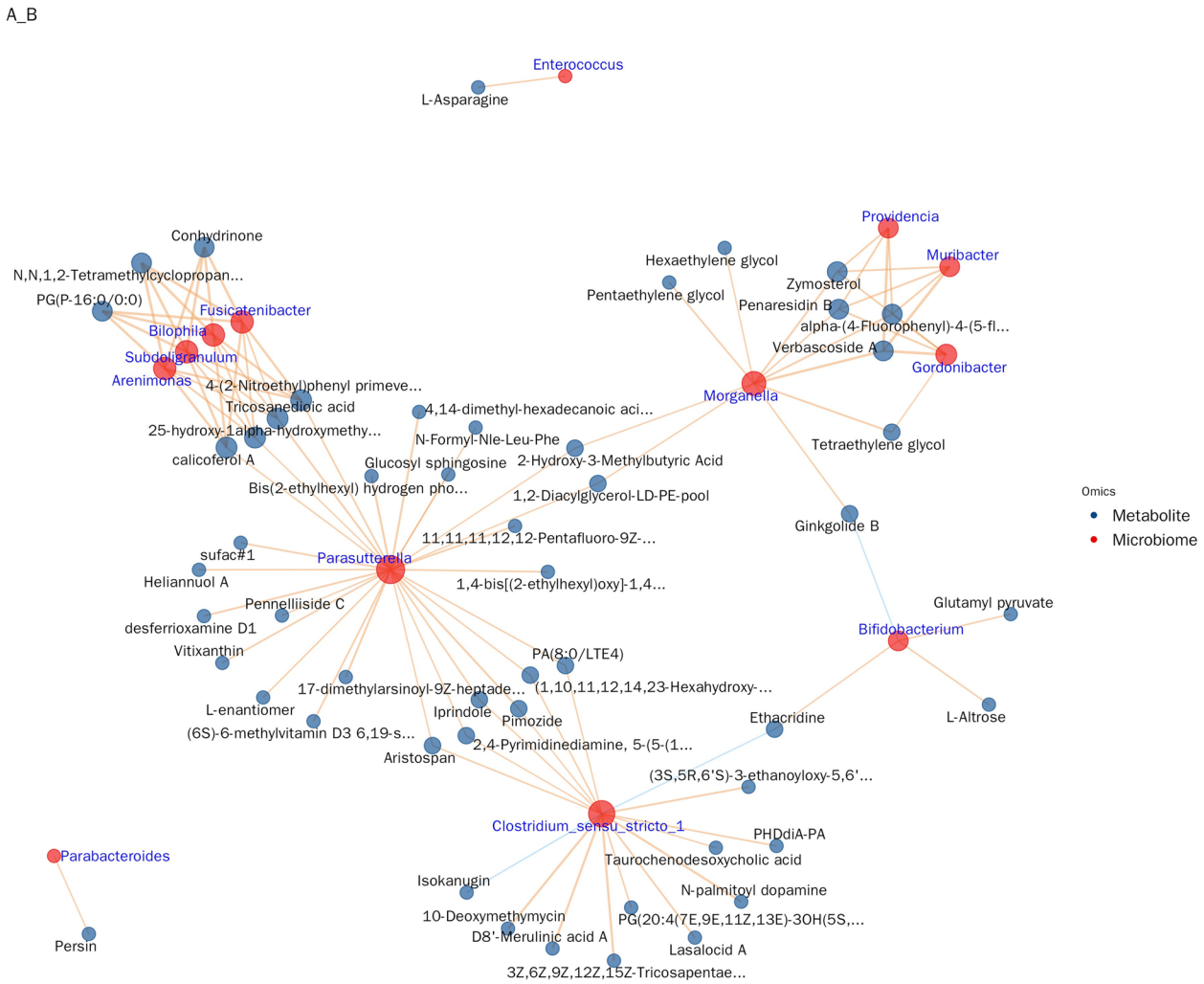

Fig. 8 Correlation analysis of differential microbiota and metabolites. The bright yellow lines represent positive correlations, while the light blue lines represent negative correlations. The thickness of the lines indicates the strength of the correlation. Red nodes represent microbes, gray nodes represent metabolites, and the size of the nodes reflects the degree of association

Abbreviations

ASV	Amplicon Sequence Variant
ACE	Abundance-based Coverage Estimator
PERMANOVA	Permutational Multivariate Analysis of Variance
PCoA	Principal Coordinates Analysis
PCA	Principal Component Analysis
OPLS-DA	Orthogonal Partial Least-Squares-Discriminant Analysis
VIP	Variable Importance of Projection

Supplementary Information

The online version contains supplementary material available at https://doi.org/10.1186/s12866-025-04020-5.

Supplementary Material 1: Figure S1 Hierarchical clustering based on the expression levels of the top 50 metabolites sorted by VIP scores. The color gradient from blue to red indicates the expression of metabolites from low to high. On the left is a dendrogram of metabolite clustering, where the closer branches indicate more similar expression patterns of all metabolites within samples.

Acknowledgements
Not applicable.

Authors' contributions
S.W: study design, data collection, and drafting of the manuscript. J.Z and M.F: data collection and analysis, article revision, and quality control. Z.D, L.L and J.X: data collection, statistical analysis, and article revision. W.Y and X.X: study design, data collection, article revision, and overall responsibility for the article. All authors read and approved the final manuscript.

Funding
This work was supported by the Nursery Program of the Affiliated Hospital of Jining Medical University [MP-MS-2021–018], the Research Project of the Attending Physician Team at the Affiliated Hospital of Jining Medical University [ZZTD-2022–004], the Talent Development Program of Affiliated Hospital of Jining Medical University [2023-yxyc-004], and the Key Research and Development Program of Jining [2024YXNS241].

Data availability
The datasets generated and analysed during the current study are available in the Genome Sequence Archive (Genomics, Proteomics & Bioinformatics 2021)

in National Genomics Data Center (Nucleic Acids Res 2022), China National Center for Bioinformation/Beijing Institute of Genomics, Chinese Academy of Sciences (GSA: CRA016722) that are publicly accessible at https://ngdc.cncb.ac.cn/gsa/browse/CRA016722.

Declarations

Ethics approval and consent to participate
This study was reviewed and approved by academic ethical committee in Affiliated Hospital of Jining Medical University and conducted in accordance with Good Clinical Practice and the principles and rules of the Declaration of Helsinki. The participants provided the written informed consent to participate in this study.

Consent for publication
Not applicable.

Competing interests
The authors declare no competing interests.

Received: 27 April 2024 Accepted: 2 May 2025
Published online: 28 May 2025

References

1. Xiang H, Han J, Ridley WE, et al. Horseshoe abscess: Perianal and giant abdominal abscess. J Med Imaging Radiat Oncol. 2018;62(S1):81–91.
2. De Souza NS, Santos DRd, Westphalen AP, et al. Fournier's gangrene by perianal abscess. J Coloproctology. 2020;40:334–8.
3. Pearce L, Newton K, Smith SR, et al. Multicentre observational study of outcomes after drainage of acute perianal abscess. Br J Surg. 2016;103:1063–8.
4. Khan MTA, Patnaik R, Huang JY, et al. Leukopenia is an independent risk factor for early postoperative complications following incision and drainage of anorectal abscess. Colorectal Dis. 2023;25(4):717–27.
5. Christison-Lagay ER, Hall JF, Wales PW, et al. Nonoperative management of perianal abscess in infants is associated with decreased risk for fistula formation. Pediatrics. 2007;120:e548–52.
6. Rosen NG, et al. The nonoperative management of fistula-in-ano. J Pediatr Surg. 2000;35:938–9.
7. Yin W, Li Y, Zhang J, et al. Natural course of perianal abscess in infants: a real-world study. Sci Rep. 2023;13:18416.
8. Domenico M, Ballini A, Boccellino M, et al. The Intestinal Microbiota May Be a Potential Theranostic Tool for Personalized Medicine. J Pers Med. 2022;12:523.
9. Lazar V, Ditu LM, Pircalabioru GG, et al. Gut Microbiota, Host Organism, and Diet Trialogue in Diabetes and Obesity. Front Nutr. 2019;6:21.
10. Shaler CR, Parco AA, Elhenawy W, et al. Psychological stress impairs IL22-driven protective gut mucosal immunity against colonising pathobionts. Nat Commun. 2021;12:6664.
11. Zhang L, Jing J, Han L, et al. Characterization of gut microbiota, metabolism and cytokines in benzene-induced hematopoietic damage. Ecotoxicol Environ Saf. 2021;228:112956.
12. Pham VT, Dold S, Rehman A, et al. Vitamins, the gut microbiome and gastrointestinal health in humans. Nutr Res. 2021;95:35–53.
13. Yin H, Luo B, Wang Q, et al. Differences in Gut Microbiota between Healthy Individuals and Patients with Perianal Abscess before and after Surgery. Mediators Inflamm. 2023:1165916.
14. Pärtty A, Luoto R, Kalliomäki M, et al. Effects of Early Prebiotic and Probiotic Supplementation on Development of Gut Microbiota and Fussing and Crying in Preterm Infants: A Randomized, Double-Blind. Placebo-Controlled Trial J Pediatr. 2013;163:1272–7.
15. Madan JC, Hoen AG, Lundgren SN, et al. Association of cesarean delivery and formula supplementation with the intestinal microbiome of 6-week-old infants. JAMA Pediatr. 2016;170:212–9.
16. Qin J, Li R, Raes J, et al. A human gut microbial gene catalogue established by metagenomic sequencing. Nature. 2010;464:59–65.
17. Crost EH, Coletto E, Bell A, et al. Ruminococcus gnavus: friend or foe for human health. FEMS Microbiol Rev. 2023;47:fuad014.
18. Coletto E, Latousakis D, Pontifex MG, et al. The role of the mucin- glycan foraging Ruminococcus gnavus in the communication between the gut and the brain. Gut Microbes. 2022;14:2073784.
19. Willing BP, Dicksved J, Halfvarson J, et al. A pyrosequencing study in twins shows that GI microbial profiles vary with inflammatory bowel disease phenotypes. Gastroenterology. 2010;139:1844–54.
20. Shin NR, Whon TW, Bae JW. Proteobacteria: microbial signature of dysbiosis in gut microbiota. Trends Biotechnol. 2015;33:496–503.
21. Blasco-Baque V, Coupé B, Fabre A, et al. Associations between hepatic miRNA expression, liver triacylglycerols and gut microbiota during metabolic adaptation to high-fat diet in mice. Diabetologia. 2017;60:690–700.
22. Fremder M, Kim SW, Khamaysi A, et al. A transepithelial pathway delivers succinate to macrophages; thus, perpetuating their proinflammatory metabolic state. Cell Rep. 2021;36:109521.
23. Harber KJ, Goede KE, Verberk SGS, et al. Succinate is an inflammation-induced immunoregulatory metabolite in macrophages. Metabolites. 2020;10:372.
24. Keiran N, Ceperuelo-Mallafré V, Calvo E, et al. SUCNR1 controls an anti-inflammatory program in macrophages to regulate the metabolic response to obesity. Nat Immunol. 2019;20:581–92.
25. Haskó G, Sitkovsky MV, Szabó C. Immunomodulatory and neuroprotective effects of inosine. Trends Pharmacol Sci. 2004;25:152–7.
26. Lee JS, Wang RX, Alexeev EE, et al. Hypoxanthine is a checkpoint stress metabolite in colonic epithelial energy modulation and barrier function. J Biol Chem. 2018;293:6039–51.
27. Li X, Zhang ZH, Zabed HM, et al. An Insight Into the Roles of Dietary Tryptophan and Its Metabolites in Intestinal Inflammation and Inflammatory Bowel Disease. Mol Nutr Food Res. 2021;65:e2000461.
28. Li X, Zhang B, Hu Y, et al. New Insights Into Gut-Bacteria-Derived Indole and Its Derivatives in Intestinal and Liver Diseases. Front Pharmacol. 2021;12:769501.
29. Zhang B, Jiang M, Zhao J, et al. The Mechanism Underlying the Influence of Indole-3-Propionic Acid: A Relevance to Metabolic Disorders. Front Endocrinol. 2022;13:841703.
30. Jeffery LE, Wood AM, Qureshi OS, et al. Availability of 25-hydroxyvitamin D(3) to APCs controls the balance between regulatory and inflammatory T cell responses. J Immunol. 2012;189:5155–64.
31. White JH. Emerging Roles of Vitamin D-Induced Antimicrobial Peptides in Antiviral Innate Immunity. Nutrients. 2022;14:284.
32. Tibbetts AS, Appling DR. Compartmentalization of Mammalian folate-mediated one-carbon metabolism. Annu Rev Nutr. 2010;30:57–81.
33. Stover PJ. One-carbon metabolism-genome interactions in folate-associated pathologies. J Nutr. 2009;139:2402–5.
34. Forman HJ, Zhang H, Rinna A. Glutathione:overview of its protective roles, measurement, and biosynthesis. Mol Aspects Med. 2009;30:1–12.
35. García-Giménez JL, Markovic J, Dasí F, et al. Nuclear glutathione. Biochim Biophys Acta. 1830;2013:3304–16.
36. Pallardó FV, Markovic J, García JL, et al. Role of nuclear glutathione as a key regulator of cell proliferation. Mol Aspects Med. 2009;30:77–85.

Publisher's Note